Online Submissions: wjg.wjgnet.com
www.wjgnet.com
wjg@wjgnet.com

*World J Gastroenterol* 2007 September 28; 13(36): 4891-4896
***World Journal of Gastroenterology*** ISSN 1007-9327


*CLINICAL RESEARCH*

# Ferucarbotran *versus* Gd-DTPA-enhanced MR imaging in the detection of focal hepatic lesions

Wei-Zhong Cheng, Meng-Su Zeng, Fu-Hua Yan, Shen-Xiang Rao, Ji-Zhang Shen, Cai-Zhong Chen, Shu-Jie Zhang, Wei-Bin Shi

Wei-Zhong Cheng, Meng-Su Zeng, Fu-Hua Yan, Shen-Xiang Rao, Ji-Zhang Shen, Cai-Zhong Chen, Shu-Jie Zhang, Wei-Bin Shi, Department of Radiology, Zhongshan Hospital, Fudan University and Department of Medical Imaging, Shanghai Medical School, Fudan University, Shanghai 200032, China
Correspondence to: Meng-Su Zeng, Department of Radiology, Zhongshan Hospital, 180 Fenglin Rd, Shanghai 200032, China. zms@zshospital.net
Telephone: +86-21-64041990-2130 Fax: +86-21-64037258
Received: March 27, 2007 Revised: May 12, 2007

## Abstract

**AIM:** To evaluate the efficacy of ferucarbotran-enhanced MR imaging in the detection of focal hepatic lesions compared to plain and Gd-DTPA-enhanced MR imaging.

**METHODS:** Fifty-nine patients with suspected focal hepatic lesions were admitted to the study. Plain MR imaging (FSE $T_2$WI with fat suppression and GRE $T_1$WI sequences) and Gd-DTPA dynamic enhanced MR of the liver were initially performed followed by ferucarbotran-enhanced MR imaging 48 h later (including GRE $T_1$WI, FSE $T_2$WI with fat suppression, and GRE $T_2$*WI sequences). Images were reviewed independently by three observers. Results were correlated with surgery and pathologic examination or reference examination, and sensitivity was statistically calculated for the different MR imaging sequences.

**RESULTS:** Among all confirmed lesions ($n$ = 133), ferucarbotran-enhanced MR imaging revealed 130 lesions on FSE $T_2$WI with fat suppression, 115 lesions on dynamic $T_1$WI GRE, and 127 lesions on GRE $T_2$*WI. Pre-contrast MR imaging revealed only 84 lesions on GRE $T_1$WI and 106 lesions on FSE $T_2$WI with fat suppression, while Gd-DTPA dynamic enhanced GRE $T_1$WI revealed 123 lesions. For 44 micro-lesions (< 1.0 cm) in all patients the detection rates were as follows: ferucarbotran-enhanced FSE $T_2$WI with fat suppression, 93.2% (41/44); ferucarbotran-enhanced GRE $T_2$*WI, 88.6% (39/44); Gd-DTPA dynamic-enhanced GRE $T_1$WI, 79.5% (35/44); pre-contrast FSE $T_2$WI with fat suppression, 54.5% (24/44); and pre-contrast GRE $T_1$WI, 34.1% (15/44). In detecting micro-lesions, statistically significant difference was found for Ferucarbotran-enhanced FSE $T_2$WI with fat suppression and GRE $T_2$*WI sequences compared to the other sequences ($P$ < 0.05).

**CONCLUSION:** Ferucarbotran-enhanced FSE $T_2$WI with fat suppression and GRE $T_2$*WI sequences are superior in detecting micro-lesions (< 1 cm) in comparison with plain and Gd-DTPA dynamic-enhanced MR imaging.



**Key words:** Liver disease; Contrast media; Superparamagnetic iron oxide; Magnetic resonance imaging

Cheng WZ, Zeng MS, Yan FH, Rao SX, Shen JZ, Chen CZ, Zhang SJ, Shi WB. Ferucarbotran *versus* Gd-DTPA-enhanced MR imaging in the detection of focal hepatic lesions. *World J Gastroenterol* 2007; 13(36): 4891-4896

http://www.wjgnet.com/1007-9327/13/4891.asp

## INTRODUCTION

The detection of focal liver lesions in patients with liver cancer is a very important challenge because failure to detect cancerous lesions can have major clinical consequences. High accuracy in liver cancer detection can improve the efficacy of treatment, including partial hepatectomy, liver transplantation, radiofrequency ablation, percutaneous ethanol injection, transarterial chemoembolization, or (commonly) a combination of these methods[1-5]. Currently, magnetic resonance (MR) is increasingly used in the detection of hepatic lesions[6]. With the use of conventional extracellular contrast agents such as gadolinium chelates, analysis of enhancement patterns on T1-weighted dynamic imaging during the different vascular phases is an important tool in the detection and characterization of focal hepatic lesions. Post-contrast imaging has been shown to be superior to conventional plain MR imaging in detecting hepatic lesions[7]. It is known, however, that 40%-60% of cancer nodules, especially those in cirrhotic liver that are smaller than 10 mm, are missed at ultrasonography (US), computed tomography (CT)[8], and MR[9]. Given this background, a possible solution to this problem is the use of liver-specific MR contrast materials: that is, agents that are targeted to either the hepatocytes or the Kupffer cells. Ferucarbotran is available as a new superparamagnetic iron oxide (SPIO) agent for liver imaging in most European countries and some Asian countries[10,11]. The present study was designed

as an open-label, within-patient comparison of the diagnostic performance of non-enhanced, gadolinium-enhanced, and ferucarbotran-enhanced MR imaging, in terms of lesion detection and characterization according to the Phase Ⅲ clinical trial of ferucarbotran in China. This article is mainly concerned with evaluating efficacy in the detection of hepatic lesions.

## MATERIALS AND METHODS

### Patients

The study protocol was approved by the Zhongshan Hospital Ethics Committee. A total of 59 patients (40 men, 19 women; mean age, 48.9 year; age range, 26-68 year) with at least one suspected focal hepatic lesion were enrolled in the study and received test contrast material between December 2003 and July 2004. Each patient gave written or witnessed informed consent and was evaluated for eligibility. Each patient underwent a reference-standard examination. The best method to confirm imaging findings-that is, pathologic confirmation-was unavailable for every patient in this study.

### Contrast material

Ferucarbotran (Resovist, Schering, Berlin, Germany) was preloaded into a 2.25 mL connecting intravenous tube (Connection Tubing; Clinico, Bad Hersfeld, Germany) and manually injected as a bolus through a filter with 5-μm pore size; the connecting catheter was flushed with 10 mL of saline solution within 3 s of injection (injection rate, approximately 2-3 mL/s). Patients with a body weight of 60 kg or more received 1.4 mL of ferucarbotran, while those with a body weight of less than 60 kg received 0.9 mL (range, 7.0-12.9 μmol iron/kg); 1 mL ferucarbotran contains 28 mg of iron. Gd-DTPA (Magnevist, Schering, Erlangen, Germany) was manually administered as an intravenous bolus injection at a dose of 0.2 mL/kg (corresponding to 0.1 mmol/kg) with a flow rate of 2-3 mL/s.

### MR imaging protocol

MR imaging was performed with a superconducting magnet operating at 1.5T (Signa, GE Medical Systems, Milwaukee, USA). The imaging protocol consisted of pre- and post-contrast imaging at 25, 60, 180, and 480 s after the administration of each contrast material, with an interval of 48 h between the injection of each. Every examination consisted of T2-weighted fast spin-echo (FSE) with fat suppression, T1-weighted fast multiplanar spoiled gradient-recalled (SPGR), and T2* GRE sequences (Table 1). The imaging factors were the same for all patients, and all sequences were performed before and after Gd-DTPA contrast agent and ferucarbotran administration.

### Imaging assessment

According to the surgical and pathologic confirmation or reference examination, all images from the MR imaging sequences were interpreted independently by three radiologists; the number of lesions was then calculated, excluding cysts. Consensus reading was necessary to ensure that both observers assessed the same lesion. Lesions were divided into three groups according to lesion size (< 1 cm, 1-3 cm, > 3 cm).

### Statistical analysis

The detection rates for the different sequences (FSE $T_2$WI with fat suppression, GRE $T_1$WI, and GRE $T_2$*WI) were compared using Pearson's chi-square test and the Fisher exact probability test. $P < 0.05$ was considered to indicate statistical significance.

## RESULTS

According to pathologic confirmation and the reference examinations, a total of 133 lesions were present among the subjects (85 lesions were confirmed by pathology; 75 hepatocellular carcinoma lesions, 35 metastatic lesions, 7 dysplastic nodules, 6 hemangiomas, 5 cases of focal nodular hyperplasia, 2 tuberculomas, 1 inflammatory pseudotumor, 2 angioleiomyolipomas). Twenty-one lesions were larger than 3.0 cm, 68 were 1-3 cm, and 44 were smaller than 1 cm. On ferucarbotran-enhanced MR imaging, FSE $T_2$WI with fat suppression revealed 130 lesions, dynamic $T_1$WI GRE revealed 115 lesions, and GRE $T_2$*WI revealed 127 lesions (Figure 1 A-H). On pre-contrast MR imaging, GRE $T_1$WI revealed only 84 lesions and FSE $T_2$WI with fat suppression revealed 106 lesions. Gd-DTPA dynamic-enhanced GRE $T_1$WI revealed 123 lesions (Table 2). Three lesions were not found by any observer on any sequence: All were smaller than 0.8 mm in diameter and were metastases from mammary adenocarcinoma and colorectal cancer. In another patient, a 0.3 mm-diameter subcapsular metastasis was detected only by ferucarbotran-enhanced FSE (Figure 2A-F).

Table 2 shows the detectability among 44 micro-lesions (< 1.0 cm) for all patients as follows: ferucarbotran-enhanced FSE $T_2$WI with fat suppression, 93.2% (41/44); ferucarbotran-enhanced GRE $T_2$*WI, 88.6% (39/44); Gd-DTPA dynamic-enhanced GRE $T_1$WI, 79.5% (35/44); pre-contrast FSE $T_2$WI with fat suppression, 54.5% (24/44); and pre-contrast GRE $T_1$WI, 34.1% (15/44). The detectability of ferucarbotran-enhanced FSE $T_2$WI with fat suppression and ferucarbotran-enhanced GRE $T_2$*WI sequences was significantly greater than that of the other sequences ($P < 0.01$).

## DISCUSSION

Ferucarbotran contains superparamagnetic iron oxide nanoparticles (maghemite [γ-$Fe_2O_3$] and magnetite [γ-$Fe_3O_4$]) coated with a carboxydexrean shell, and was developed as a new intravenous liver-specific contrast agent. Its T1 relaxivity is 25.4 mmol/L per second, with T2 relaxivity of 151.0 mmol/L. second. The blood half-life is similar to that of ferumoxides (another SPIO agent), but the mean particle size is smaller (60 nm)[10,11]. Ferucarbotran is taken up by reticuloendothelial system (RES) cells in the liver, spleen, bone marrow, and lymph nodes. Hydrolytic enzymes degrade intracellular SPIO particles causing a loss of R2 relaxivity as the iron loses its

**Table 1 MR sequences and parameters**

| Sequence | TR | TE | NEX | Matrix | FOV (cm) | Thickness | Intersection gap (mm) | Flip angle (mm) |
|---|---|---|---|---|---|---|---|---|
| T2-FSE/TSE with fat suppression | 3333-4000 | 98 | 2 | 256 × 160 | 36 × 36 | 8 | 2 | - |
| GRE $T_1$WI | 150 | 2 | 1 | 256 × 128 | 36 × 36 | 8 | 2 | 90° |
| GRE $T_2$*WI | 150 | 11.5 | 1 | 256 × 160 | 36 × 36 | 8 | 2 | 10° |

**Table 2 Comparative analysis of lesion detection for 133 lesions in 59 patients using pre-contrast, ferucarbotran-enhanced, and Gd-DTPA-enhanced sequences**

| Sequence | *n* (%) | | |
|---|---|---|---|
| | < 1 cm (*n* = 44 ) | 1-3 cm (*n* = 68) | > 3 cm (*n* = 21 ) |
| 1 Pre-contrast T1WI GRE | 15 (34.1)[b] | 48 (70.6)[b] | 21 (100.0) |
| 2 Pre-contrast FSE $T_2$WI with fat suppression | 24 (54.5)[b] | 61 (89.7) | 21 (100.0) |
| 3 Dynamic Gd-DTPA-enhanced T1WI GRE | 35 (79.5)[a] | 67 (98.5) | 21 (100.0) |
| 4 Dynamic ferucarbotran-enhanced T1WI GRE | 32 (72.7) | 62 (91.2) | 21 (100.0) |
| 5 Delayed ferucarbotran-enhanced FSE $T_2$WI with fat suppression | 41 (93.2) | 68 (100) | 21 (100.0) |
| 6 Delayed ferucarbotran-enhanced GRE $T_2$*WI | 39 (88.6) | 67 (98.5) | 21 (100.0) |

[a]$P < 0.05$, [b]$P < 0.01$, *vs* (5), (6).

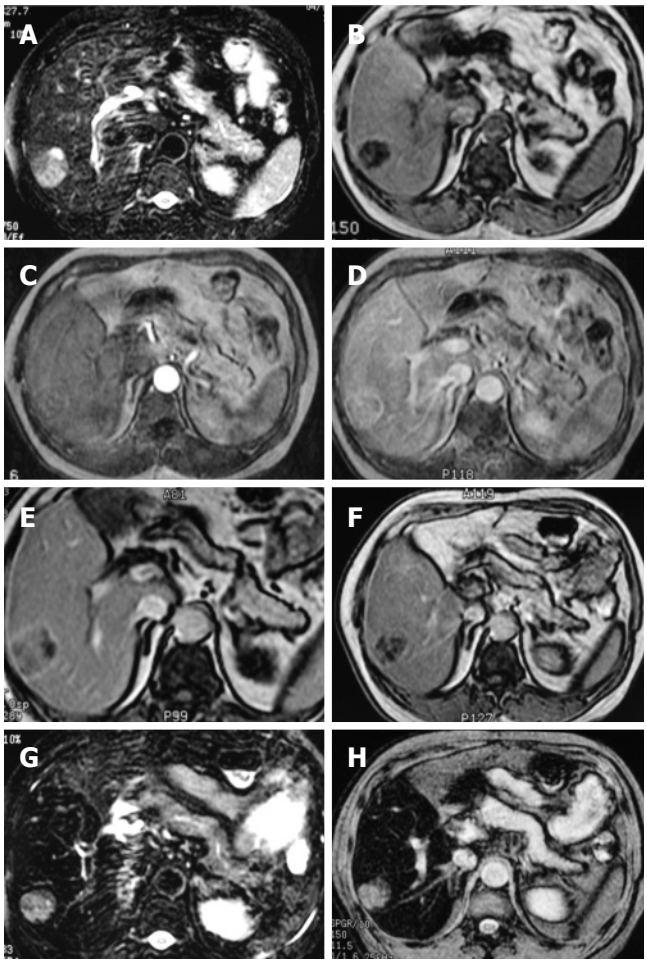


**Figure 1** Images of HCC. **A**: The lesion appears hyperintense on the pre-contrast T2WI FSE image; **B**: The lesion appears hypointense on the pre-contrast T1WI GRE image; **C**: The lesion enhances inhomogeneously during the hepatic arterial phase; **D**: Ring-enhancement is observed during the portal venous phase; **E**, **F**: Dynamic T1WI GRE images obtained after administration of ferucarbotran show ring-enhancement of an asymmetric moderately hyperintense lesion; **G**, **H**: A markedly hyperintense lesion with surrounding hypointense liver parenchyma is shown during the accumulation phase on ferucarbotran-enhanced T2WI and T2*WI images.

crystalline structure [12]. Within minutes of administration, 80% of the injected dose of SPIO agent efficiently accumulates in the liver, while approximately 5%-10% of the injected dose accumulates in the spleen[13-15]. On T2-weighted sequences there is a marked decrease in the signal intensity of normal liver and spleen; because malignant tumor tissue typically lacks a substantial number of Kupffer cells or has a lower activity of phagocytic cells, it appears as hyperintense/bright lesions that are contrasted against the hypointense/black liver[11,16].

In the detection of micro-lesions (< 1.0 cm) in the present study, delayed T2-weighted ferucarbotran-enhanced FSE with fat suppression and $T_2$*-weighted ferucarbotran-enhanced GRE provided higher sensitivity in MR imaging than pre-contrast (T1-weighted GRE) images (93.2% and 88.6%, respectively, *vs* 34.1%). More lesions were detected on T2-weighted ferucarbotran-enhanced FSE than on dynamic Gd-DTPA-enhanced images in 16%-20% of our patients. It had statistically significant difference in detecting micro-lesions ($P = 0.021$), which is in agreement with previous studies[11,16-18]. In the present study, even a 0.3 mm-diameter metastasis was detected by T2-weighted ferucarbotran-enhanced FSE with fat suppression. The loss of liver parenchyma signal intensity after ferucarbotran administration improves lesion-to-liver contrast, which in turn improves detection (especially in micro-lesions), visualization, delineation, and overall diagnostic confidence[19] (Figure 3A-D). Although diagnostic confidence is a subjective parameter, it is relevant in the clinical situation because a radiologist must determine the confidence with which findings observed on images are correct. Evaluation of diagnostic certainty was also recommended by Thornbury in his six-tier model of efficacy[20]. Diagnostic confidence conceptualizes the diagnostic thinking efficacy (one tier of the Thornbury model) and links the technical and diagnostic efficacy of a contrast agent to the therapy of the patient. Higher accuracy in liver cancer detection potentially changes the clinical treatment of patients with liver cancer. The report of Ros *et al* states that the proportionate change in clinical treatment was as high as 59% after examination using SPIO-enhanced MR[21]. For detection of lesions larger than 1 cm, there was no significant difference among the findings of the different sequences (excluding pre-

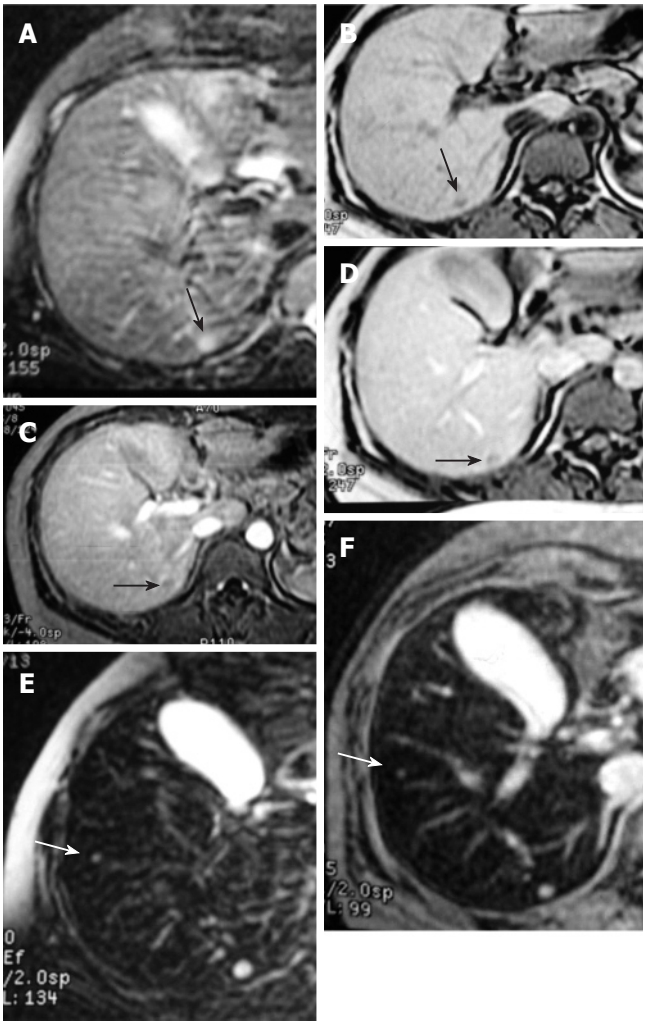


**Figure 2** Liver metastasis from mammary adenocarcinoma. **A**, **B**: Only one lesion (black arrow) was found on the pre-contrast T2WI and T1WI GRE images; **C**, **D**: Only one lesion (black arrow) was found on dynamic T1WI GRE images obtained after administration of Gd-DTPA; **E**, **F**: An additional small metastasis (0.3 mm, white arrow) was detected on T2WI and T2*WI images during the accumulation phase.

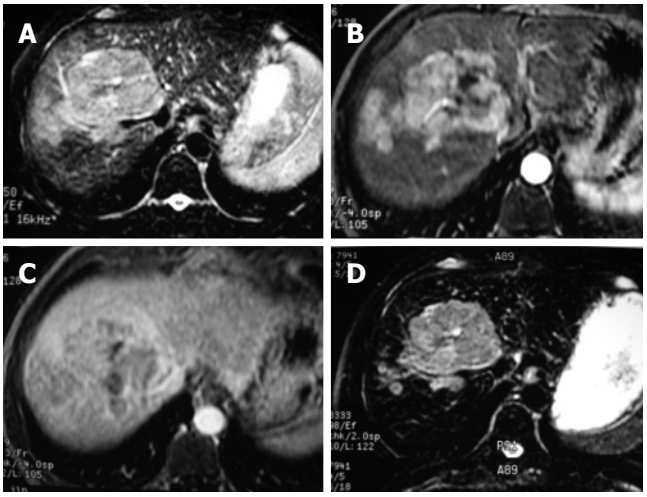


**Figure 3** HCC image. **A**: The lesion appears hyperintense on the pre-contrast T2WI FSE image, but is not clearly delineated; **B**: The lesion is markedly enhanced during the hepatic arterial phase; **C**: The lesion appears hypointence during the portal venous phase, but is not clearly delineated; **D**: The main lesion and satellite nodules are clearly delineated from the surrounding hypointense liver parenchyma on the ferucarbotran-enhanced T2WI image during the accumulation phase.

contrast sequences); however, diagnostic confidence was determined for the same reason as that described above.

Ferucarbotran is an SPIO agent that can be injected as a bolus[10]. It contains particles with smaller mean hydrodynamic diameter than that of the stock solution, which has a stronger T1-effect and longer blood half-life because of slower uptake into the RES. Previous studies using animals found that iron particles begin attaching to the Kupffer cells 3 min after administration[22]. The R1 relaxivity of ferucarbotran varies considerably within the range of diagnostically applied proton Larmor frequency (i.e., field strength); however, R1 relaxivity at 40 MHz with 12.3 mmol/L per second is still four times higher than the R1 relaxivity of low molecular gadolinium chelates. The very high R2/R1 ratio is characteristic of superparamagnetic colloids of the SPIO type. This ratio varies from 6 to 15 as the Larmor frequency increases from 10 to 40 MHz, a fact which might be in favor of the use of lower imaging fields to better utilize the T1 effect of these materials[12]. In fact, this subfraction contributes to the signal change on T1-weighted images and is the reason why the signal characteristics are comparable to those of angiographic agents with a blood-pool effect. This subfraction also explains the biexponential blood half-life of ferucarbotran, which has also been tested for its capability in contrast-enhanced MRA[23]. Enhancement increased with the degree of T1-weighting and shifted towards higher concentrations with shorter echo times. The T1 effect of ferucarbotran is a function of dose and concentration in plasma, and can be monitored during a time window in which the plasma concentration stays below a certain level depending on pulse sequence parameters. Nevertheless, in the present study, dynamic ferucarbotran-enhanced T1-weighted GRE/FLASH showed no superiority over dynamic Gd-DTPA-enhanced T1-weighted GRE/FLASH in the detection of lesions. The benefit of dynamic T1-weighted MR imaging techniques is in the characterization of lesions; however, in many respects dynamic imaging with ferucarbotran is different from that with Gd-DTPA. In dynamic T1-weighted images obtained with ferucarbotran, the signal increase is observed to be lower but longer lasting, as described by Amelie *et al*[24].

Ferucarbotran has an advantage over ferumoxides (Feridex, Advanced Magnetics; Guerbet), which is the only marketed SPIO in most countries. Although it is well known that ferumoxides have relatively high R1 values (up to four or five times higher than those of gadolinium-based contrast agents)[10,25,26], these T1 effects cannot be readily exploited for dynamic T1-weighted MR imaging. Bolus administration of ferumoxides has not been recommended because of the possible side effects (lumbar pain and cardiovascular problems, including dose-dependent hypotensive reactions) that positively correlate to the rate of injection; therefore, this compound must be administered as a slow drip infusion[13]. Ferucarbotran used in this study has few side effects[10,11] and can be given as a

rapid bolus injection. No adverse reactions were observed in any of the patients in the present study; however, as for any SPIO contrast agent, the efficacy of ferucarbotran depends on the number of Kupffer cells or their activity. For example, some well-differentiated hepatocellular carcinoma lesions still contain a certain amount of Kupffer cells and which could confuse us to make the correct diagnosis[27,28].

In conclusion, ferucarbotran is a safe contrast material for MR imaging of local liver lesions. The use of ferucarbotran-enhanced images improves diagnostic confidence and lesion detection, especially in the detection of micro lesions (< 1 cm). Ferucarbotran can be rapidly injected without clinically important adverse events, enabling dynamic MR imaging to be performed. As a dual-function and complementary MR imaging agent, ferucarbotran-enhanced images in combination with dynamic Gd-DTPA-enhanced images are helpful in improving the accuracy of differential diagnoses for focal hepatic lesions.

## COMMENTS

### Background

In patients with liver cancer, the detection of focal liver lesions is one of the most important challenges. High accuracy in liver cancer detection can improve the efficacy of treatment. It is known, however, that 40%-60% of cancer nodules, especially those that are smaller than 10 mm in cirrhotic liver, are missed on ultrasonography (US), computed tomography (CT) and magnetic resonance (MR).

### Research frontiers

Ferucarbotran, a liver-specific MR contrast material targeted to the Kupffer cells, is available as a new superparamagnetic iron oxide (SPIO) agent for liver imaging. A current research hotspot involves the evaluation of two contrast media for their efficacy in detecting hepatic lesions.

### Innovations and breakthroughs

Ferucarbotran is a safe contrast material for MR imaging of focal liver lesions. The use of ferucarbotran-enhanced images improves diagnostic confidence and lesion detection, especially in the detection of micro lesions.

### Applications

Ferucarbotran-enhanced images combined with dynamic Gd-DTPA-enhanced images aid in improving the accuracy of differential diagnosis for focal hepatic lesions.

### Terminology

SPIO agent is a liver-specific contrast agent that contains superparamagnetic iron oxide nanoparticles coated with a carboxydexrean shell. Ferucarbotran is taken up by reticuloendothelial system (RES) cells in the liver, spleen, bone marrow, and lymph nodes.

### Peer review

The effectiveness of ferucarbotran-enhanced MR imaging in the detection of hepatic lesions is known. The present study compares the diagnostic efficiency of three MR imaging sequences in patients with focal hepatic lesions. The scientific value of this manuscript is demonstrated.

## REFERENCES


1 **Zavadsky KE**, Lee YT. Liver metastases from colorectal carcinoma: incidence, resectability, and survival results. *Am Surg* 1994; **60**: 929-933
2 **Poon RT**, Fan ST. Hepatectomy for hepatocellular carcinoma: patient selection and postoperative outcome. *Liver Transpl* 2004; **10**: S39-S45
3 **Schwartz M**. Liver transplantation in patients with hepatocellular carcinoma. *Liver Transpl* 2004; **10**: S81-S85
4 **Yamamoto J**, Okada S, Shimada K, Okusaka T, Yamasaki S, Ueno H, Kosuge T. Treatment strategy for small hepatocellular carcinoma: comparison of long-term results after percutaneous ethanol injection therapy and surgical resection. *Hepatology* 2001; **34**: 707-713
5 **Llovet JM**, Bruix J. Systematic review of randomized trials for unresectable hepatocellular carcinoma: Chemoembolization improves survival. *Hepatology* 2003; **37**: 429-442
6 **Larson RE**, Semelka RC. Magnetic resonance imaging of the liver. *Top Magn Reson Imaging* 1995; **7**: 71-81
7 **Ward J**, Baudouin CJ, Ridgway JP, Robinson PJ. Magnetic resonance imaging in the detection of focal liver lesions: comparison of dynamic contrast-enhanced TurboFLASH and T2 weighted spin echo images. *Br J Radiol* 1995; **68**: 463-470
8 **Baron RL**. Detection of liver neoplasms: techniques and outcomes. *Abdom Imaging* 1994; **19**: 320-324
9 **Pauleit D**, Textor J, Bachmann R, Conrad R, Flacke S, Layer G, Kreft B, Schild H. Hepatocellular carcinoma: detection with gadolinium- and ferumoxides-enhanced MR imaging of the liver. *Radiology* 2002; **222**: 73-80
10 **Reimer P**, Rummeny EJ, Daldrup HE, Balzer T, Tombach B, Berns T, Peters PE. Clinical results with Resovist: a phase 2 clinical trial. *Radiology* 1995; **195**: 489-496
11 **Kopp AF**, Laniado M, Dammann F, Stern W, Grönewäller E, Balzer T, Schimpfky C, Claussen CD. MR imaging of the liver with Resovist: safety, efficacy, and pharmacodynamic properties. *Radiology* 1997; **204**: 749-756
12 **Josephson L**, Lewis J, Jacobs P, Hahn PF, Stark DD. The effects of iron oxides on proton relaxivity. *Magn Reson Imaging* 1988; **6**: 647-653
13 **Hamm B**, Staks T, Taupitz M, Maibauer R, Speidel A, Huppertz A, Frenzel T, Lawaczeck R, Wolf KJ, Lange L. Contrast-enhanced MR imaging of liver and spleen: first experience in humans with a new superparamagnetic iron oxide. *J Magn Reson Imaging* 1994; **4**: 659-668
14 **McLachlan SJ**, Morris MR, Lucas MA, Fisco RA, Eakins MN, Fowler DR, Scheetz RB, Olukotun AY. Phase I clinical evaluation of a new iron oxide MR contrast agent. *J Magn Reson Imaging* 1994; **4**: 301-307
15 **Weissleder R**, Stark DD, Engelstad BL, Bacon BR, Compton CC, White DL, Jacobs P, Lewis J. Superparamagnetic iron oxide: pharmacokinetics and toxicity. *AJR Am J Roentgenol* 1989; **152**: 167-173
16 **Matsuo M**, Kanematsu M, Itoh K, Ito K, Maetani Y, Kondo H, Kako N, Matsunaga N, Hoshi H, Shiraishi J. Detection of malignant hepatic tumors: comparison of gadolinium-and ferumoxide-enhanced MR imaging. *AJR Am J Roentgenol* 2001; **177**: 637-643
17 **Denys A**, Arrive L, Servois V, Dubray B, Najmark D, Sibert A, Menu Y. Hepatic tumors: detection and characterization at 1-T MR imaging enhanced with AMI-25. *Radiology* 1994; **193**: 665-669
18 **Blakeborough A**, Ward J, Wilson D, Griffiths M, Kajiya Y, Guthrie JA, Robinson PJ. Hepatic lesion detection at MR imaging: a comparative study with four sequences. *Radiology* 1997; **203**: 759-765
19 **Shamsi K**, Balzer T, Saini S, Ros PR, Nelson RC, Carter EC, Tollerfield S, Niendorf HP. Superparamagnetic iron oxide particles (SH U 555 A): evaluation of efficacy in three doses for hepatic MR imaging. *Radiology* 1998; **206**: 365-371
20 **Thornbury JR**. Eugene W. Caldwell Lecture. Clinical efficacy of diagnostic imaging: love it or leave it. *AJR Am J Roentgenol* 1994; **162**: 1-8
21 **Ros PR**, Freeny PC, Harms SE, Seltzer SE, Davis PL, Chan TW, Stillman AE, Muroff LR, Runge VM, Nissenbaum MA. Hepatic MR imaging with ferumoxides: a multicenter clinical trial of the safety and efficacy in the detection of focal hepatic lesions. *Radiology* 1995; **196**: 481-488
22 **Okon E**, Pouliquen D, Okon P, Kovaleva ZV, Stepanova

TP, Lavit SG, Kudryavtsev BN, Jallet P. Biodegradation of magnetite dextran nanoparticles in the rat. A histologic and biophysical study. *Lab Invest* 1994; **71**: 895-903

23 **Reimer P**, Allkemper T, Matuszewski L, Balzer T. Contrast-enhanced 3D-MRA of the upper abdomen with a bolus-injectable SPIO (SH U 555 A). *J Magn Reson Imaging* 1999; **10**: 65-71

24 **Lutz AM**, Willmann JK, Goepfert K, Marincek B, Weishaupt D. Hepatocellular carcinoma in cirrhosis: enhancement patterns at dynamic gadolinium- and superparamagnetic iron oxide-enhanced T1-weighted MR imaging. *Radiology* 2005; **237**: 520-528

25 **Jung CW**, Jacobs P. Physical and chemical properties of superparamagnetic iron oxide MR contrast agents: ferumoxides, ferumoxtran, ferumoxsil. *Magn Reson Imaging* 1995; **13**: 661-674

26 **Paley MR**, Mergo PJ, Torres GM, Ros PR. Characterization of focal hepatic lesions with ferumoxides-enhanced T2-weighted MR imaging. *AJR Am J Roentgenol* 2000; **175**: 159-163

27 **Imai Y**, Murakami T, Yoshida S, Nishikawa M, Ohsawa M, Tokunaga K, Murata M, Shibata K, Zushi S, Kurokawa M, Yonezawa T, Kawata S, Takamura M, Nagano H, Sakon M, Monden M, Wakasa K, Nakamura H. Superparamagnetic iron oxide-enhanced magnetic resonance images of hepatocellular carcinoma: correlation with histological grading. *Hepatology* 2000; **32**: 205-212

28 **Kim SH**, Choi D, Kim SH, Lim JH, Lee WJ, Kim MJ, Lim HK, Lee SJ. Ferucarbotran-enhanced MRI versus triple-phase MDCT for the preoperative detection of hepatocellular carcinoma. *AJR Am J Roentgenol* 2005; **184**: 1069-1076

**S- Editor** Ma N **L- Editor** Boyes A **E- Editor** Ma WH